Pergamon

SCIENCE DIRECT®

Bioorganic & Medicinal Chemistry 11 (2003) 2007–2018

BIOORGANIC & MEDICINAL CHEMISTRY

Tricyclic Quinoxalines as Potent Kinase Inhibitors of PDGFR Kinase, Flt3 and Kit

Aviv Gazit,[a,†] Kevin Yee,[†b] Andrea Uecker,[c] Frank-D. Böhmer,[c] Tobias Sjöblom,[d] Arne Östman,[d] Johannes Waltenberger,[e] Gershon Golomb,[f] Shmuel Banai,[g] Michael C. Heinrich[b] and Alexander Levitzki[a,*]

[a]*Department of Biological Chemistry, The Alexander Silberman Institute of Life Sciences, The Hebrew University of Jerusalem, Givat Ram, Jerusalem 91904, Israel*

[b]*Department of Hematology and Medical Oncology, Oregon Health and Science University Cancer Institute and Portland Veteran's Affairs Medical Center, Portland, OR 97239, USA*

[c]*Research Unit 'Molecular Cell Biology', Klinikum der Friedrich-Schiller-Universität Jena, Drackendorfer Str.1, D-07747 Jena, Germany*

[d]*The Ludwig Institute for Cancer Research, Box 595, S-751 24 Uppsala, Sweden*

[e]*Department of Internal medicine II,Ulm University Medical Center, Robert Koch Strasse 8,D89081, Germany*

[f]*School of Pharmacy, The Hebrew University of Jerusalem, Ein Karem, Jerusalem, 91904, Israel*

[g]*Department of Cardiology, Bikur Cholim Hospital POB. 492 Jerusalem 91004, Israel*

Received 22 August 2002; accepted 17 January 2003

Abstract—Here we report on novel quinoxalines as highly potent and selective inhibitors of the type III receptor tyrosine kinases PDGFR, FLT3, and KIT. These compounds, tricyclic quinoxalines, were generated in order to improve bioavailability over the highly hydrophobic bicyclic quinoxalines. Four of the highly active compounds were characterized in detail and are shown to inhibit PDGFR kinase activity of the isolated receptor as well as in intact cells in the sub-micromolar concentration range. We show that the most active inhibitor (compound **13**, AGL 2043) is ~15–20 times more potent than its isomer (compound **14**, AGL 2044). We therefore compared the three dimensional structures of the two compounds by X-ray crystallography. These compounds are also highly effective in blocking the kinase activity of FLT3, KIT, and the oncogenic protein Tel-PDGFR in intact cells. These compounds are potent inhibitors of the proliferation of pig heart smooth muscle cells. They fully arrest the growth of these cells and the effect is fully reversible. The chemical, biochemical and cellular properties of these compounds as well as the solubility properties make them suitable for development as anti-restenosis and anti-cancer agents.
© 2003 Elsevier Science Ltd. All rights reserved.

Introduction

The enhanced activity of PDGFR receptor plays a pivotal role in various cancers as well as in non-malignant diseases such as atherosclerosis, balloon injury induced restenosis and restenosis subsequent to by-pass operations. Therefore we have been targeting this receptor repeatedly for over a decade (for review see ref 1). In previous studies,[2–6] we reported on bicyclic quinoxaline derivatives as potent inhibitors of PDGF receptor tyrosine kinase. These compounds reverse the transformed phenotype of *sis* transformed cells[3] and effectively inhibit balloon injury stenosis in the pig[7] and are effective in the prophylaxis of allograft vasculopathy.[8] The best inhibitors were compounds **1** and **2** (Scheme 1) but they are highly hydrophobic. Compound **3** (Scheme 1), where a fused benzoic ring replaces the 6,7-diethyl or dimethoxy substituents was almost as good, but is even more hydrophobic. Substituents at the 2-position greatly diminished potency.[2] It seems that the 7,8-positions area is less congested and amenable to further SAR study. We therefore utilized this information for the synthesis of novel compounds attempting to achieve PDGFR kinase inhibitors with higher potency and with diminished hydrophobicity. Here we report on new and potent benzimidazole analogues, compounds **11**–**14**, which are good candidates for new agents against restenosis, neoplasia, in which PDGF,[1,8,9] FLT3[10] or KIT[11] receptors play important roles.

*Corresponding author. Tel.: +972-2-658-5404; fax: +972-2-651-2958; e-mail: levitzki@vms.huji.ac.il
†These authors contributed equally.

0968-0896/03/$ - see front matter © 2003 Elsevier Science Ltd. All rights reserved.
doi:10.1016/S0968-0896(03)00048-8

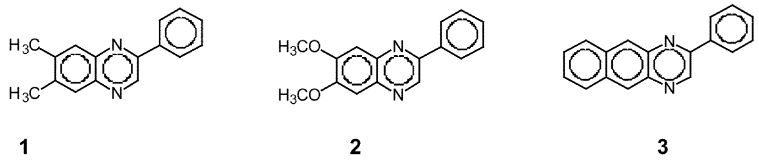

Scheme 1.

Results

Chemistry

The synthesis of the inhibitors is shown in Schemes 2 and 3. The key intermediate compound **10** was prepared as described in Scheme 2. Nitration of 1,2-dimethyl benzimidazole **5** gave a mixture containing mainly the 5-nitro isomer **6** and the 6-NO_2 isomer **7**. When nitration was performed under more drastic conditions the desired 5,6-dinitro **9** was obtained. Reaction of diamine **10** with phenyl glyoxal or thiophene glyoxal (produced in situ from the nitrone **21**) produced isomer pairs **11**, **12** and **13**, **14**, which we were able to separate through careful chromatography. To probe the influence of a more bulky and lipophilic group a ferrocenne substituent was introduced into position 3 (**18**).

Solubility properties

Compounds **11**/**12** (AGL 2033/34) and compounds **13**/**14** (AGL 2043/44) were designed in order to obtain quinoxalines with enhanced solubility in aqueous solutions as compared to the hydrophobic Compounds **11** and **12** (AG 1295/6). Indeed the imidazolo derivatives of AG 1295 seem to fulfill this aim (Table 1).

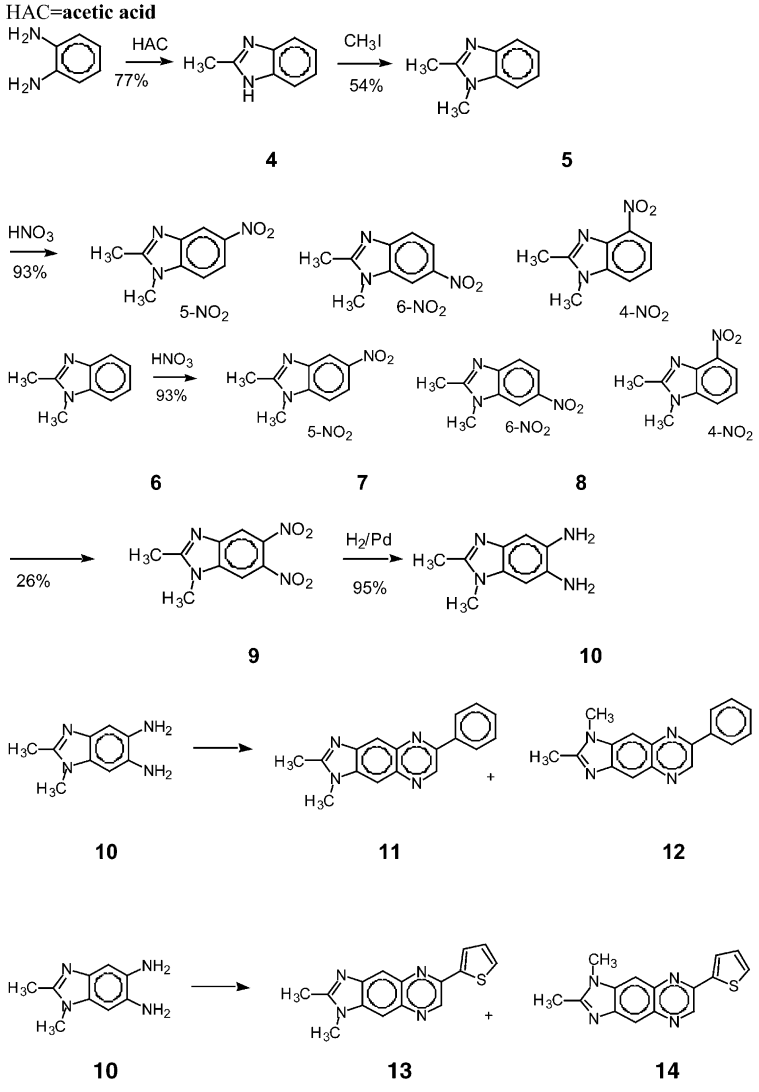

Scheme 2.

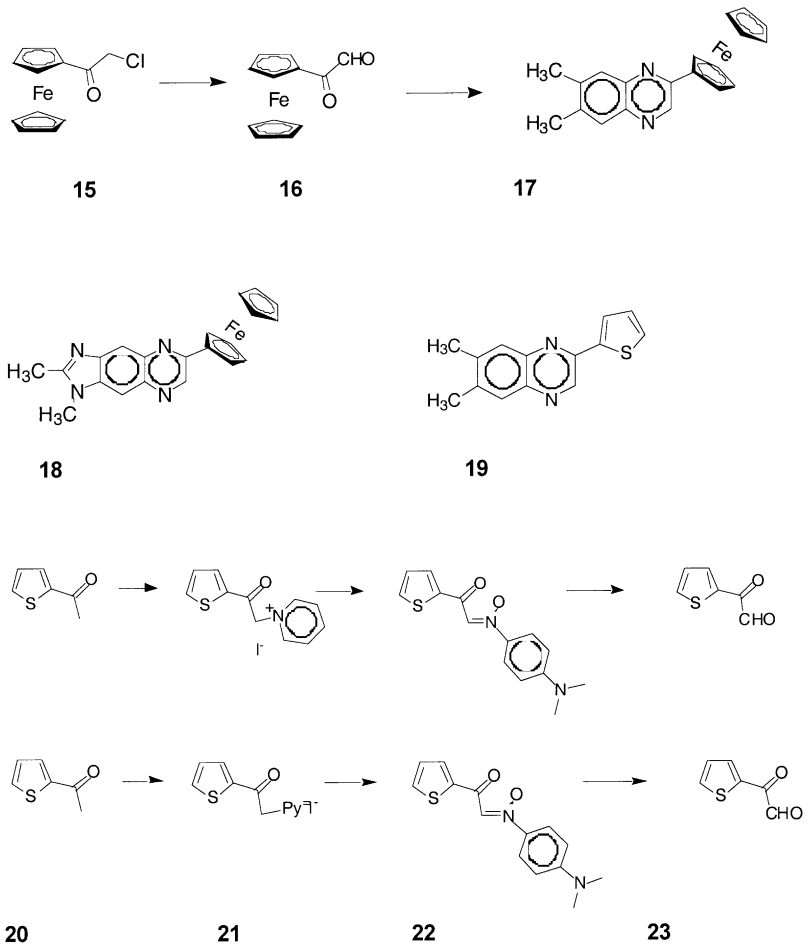

Scheme 3.

Table 1. Solubilities of compound **1** and compound **13**

Solvent	Compd **1**	Compd **13** (mg/L)
Heptane	2800	5
Water	<0.5	2

X-ray crystal structure determination

Out of the two pairs of prepared isomer inhibitors — **11**, **12** and **13**, **14** — the faster moving isomer (TLC and chromatography) was found to be about 20 times more potent than the slower moving one (see below, Table 2). Since the NMR spectra for each pair are very similar and do not allow an unequivocal assignment, we sought to establish the correct assignment through an X-ray study of the thiophene substituted isomer pair, **13** and **14** (Schemes 4 and 5 respectively). Single **13** and **14** crystals were grown through slow evaporation of acetonitrile solution.

13. $C_{15}H_{12}N_4S$, Space group $P2_1$; $a=10.384(2)$, $b=19.081(4)$, $c=6.618(1)$; $\alpha=90.00$, $\beta=107.10.00$, $\gamma=90.00$; $V(A^3)=1307.7(5)$; $Z=4$; density $=1.42$ g cm^{-3}; μ (CuK_α) $=21.46$. A total of 2007 unique reflections were measured. The number of reflections with $I>3\sigma$ was 1688. $R=0.049$, $R_w=0.062$.

Table 2. Activity of tricyclic quinoxalines against PDGFR, Src and EGFR

Compd	AG/AGL number	PDGFR	Src	EGFR	PDGFR
		Intact cell assays IC_{50} (μM)			Cell-free assay IC_{50} (nM)
1	AG1295	0.4±0,07	>30	>100	40±3.3[a]
2	AG1296	0.8±0.11	>30	>100	40±2.3[a]
3	AG1385	14.0±1.6	>30	>100	802±20[a]
11	AGL2033	0.7±0.09	>30	>30	70±6.6[b]
12	AGL2034	15.6±1.4	>30	>30	1150±28[b]
13	AGL2043	0.8±0.09	>30	>30	90±8.2[b]
14	AGL2044	13.2±0.08	>30	>30	1200±98[b]
17	AGL1989	25.0±3.1	>30	>30	ND
18	AGL1991	20.0±2.5	>30	>30	ND
19	AGL1990	1.0±0.11	20	>30	ND

ND, not determined. The IC_{50} values are for the inhibition of autophosphorylation of PTKs depicted in the table using the methodologies described in refs 3 and 4. Determinations were carried out in triplicates in three separate experiments. Data is presented as the average of three separate experiments with standard error of the mean.
[a]With membranes from Swiss 3T3 cells. Data taken from ref 3.
[b]With purified PDGFβ-receptor.

14. $C_{15}H_{12}N_4S$, $1.5H_2O$, Space group $P2_1/c$; $a=7.261(3)$, $b=17.789(3)$, $c=23.293(4)$; $\alpha=90.00$, $\beta=98.00$, $\gamma=90.00$; $V(A^3)=2979(1)$; $Z=8$; density $=1.370$ g cm^{-3}; μ (CuK_α) $=20.074$. A total of 4560 unique reflections were measured. The number of reflections with $I>3\sigma$ was 3621. $R=0.051$, $R_w=0.074$.

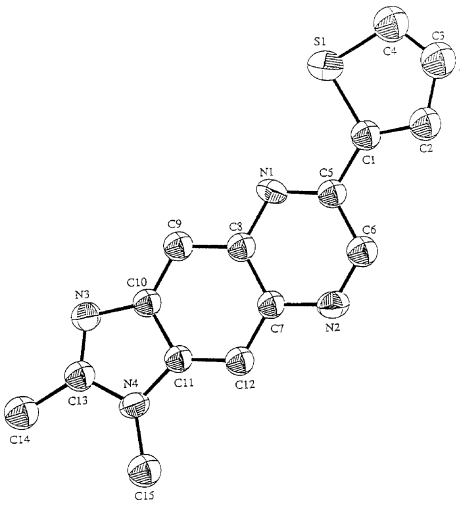

Scheme 4.

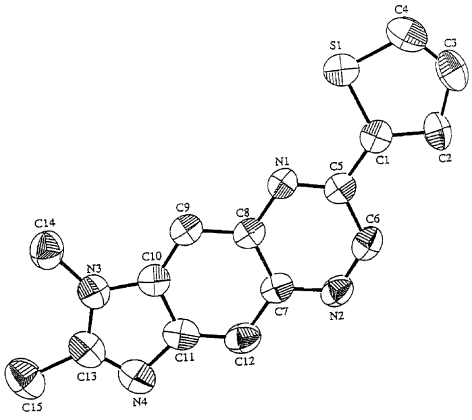

Scheme 5.

Aromatic bond lengths ranged between 1.38 and 1.43 Å. Distances are measured in angstroms. All other angles ranged between 117.1 and 123.9°. Angles are measured in degrees. Estimated standard deviations for least significant figure are given in parentheses. The unit cell contained two **13** molecules whose similar parameters were solved.

All the aromatic bond lengths ranged between 1.38 and 1.43 Å. Distances are measured in angstroms. All other angles ranged between 117.1 and 123.9°. Estimated standard deviations for the least significant figure are given in parentheses. Full data can be supplied upon request.

The unit cell contained two **14** molecules whose similar parameters were solved.

Selectivity of the tricyclic quinoxalines

We tested the selectivity of the tricyclic quinoaxlines as we described for the bicyclic compounds.[2,3] As was the case with compounds **1** and **2**, the tricyclic quinoxalines found to be the most selective against PDGFR (**11**, **12**, **13** and **14**) do not inhibit PKA at concentrations below 100 μM; similar results were obtained for PKB/c-Akt, EGFR, Src kinase, IGF-1R and VEGFR. These kinases were not inhibited by these compounds at concentrations up to 30 μM (data not shown), either in a cell free assay or in a cellular assay (Table 2 and data not shown).

Cellular activities of the kinase inhibitors

From the compounds we prepared, compounds **11**–**14** (AGL 2033, AGL 2034, AGL 2043 and AGL 2044) are the most potent inhibitors of PDGFR and TEL-PDGFR kinase in intact cells (Table 2 and Figs 1 and 2). These experiments show that compound **11** is better than its isomer **12** and that compound **13** is better than its isomer **14**. Compound **13** (AGL 2043) and compound **14** (AGL 2044) were also tested as inhibitors of pig heart smooth muscle cell proliferation using the same assays as described before for compound **1**[7] (see Experimental). Figure 3 shows that compound **13** and compound **14** are very potent inhibitors of smooth muscle cell proliferation where the potency ranking is compound **13** > compound **14** > compound **1**. It can also be seen that all three tyrphostins act reversibly on the smooth muscle cells, suggesting that their effect is cytostatic and non-cytotoxic to these cells. Compound **13** was recently also shown to inhibit balloon induced stenosis in the left anterior descending pig coronary artery of the pig heart, when applied locally (unpublished experiments), with efficacy greater than that described for compound **1** (AG 1295).[7]

We hypothesized that the activity of PDGFR kinase inhibitors could extend to other members of the Type III tyrosine kinase receptor family and therefore tested them in cellular assays for FLT3 and KIT. Compounds **11**–**14** were indeed found to be potent inhibitors of FLT3 and KIT kinase with relative potencies similar to each compound's effects on PDGFR (Figs 4 and 5). Compound **11** was superior to **12** and compound **13** was better than **14** similar to the situation for PDGFR. The compounds were capable of inhibiting the proliferation of cells dependent on wild type or mutant FLT3 signaling in dose ranges (IC_{50} = 1–3 μM) consistent with those seen for kinase inhibition in intact cells. Proliferation could be restored by the addition of an alternative growth factor (data not shown). These findings support the notion that compounds **11**–**14** are non-toxic but further work is needed to establish their toxicity profile in vivo.

Discussion

In the last decade, several potent inhibitors classes for tyrosine kinases were discovered. These inhibitors are hetero bicyclic or tricyclic compounds whose core bears close resemblance to adenine. Not surprisingly, they all bind at the ATP site of the tyrosine kinases. This resemblance is especially evident in pyrrolo or pyrazolo pyimidine family of Src family inhibitors[12,13] and the quinazolines inhibitors of EGF receptor, with their 1,3

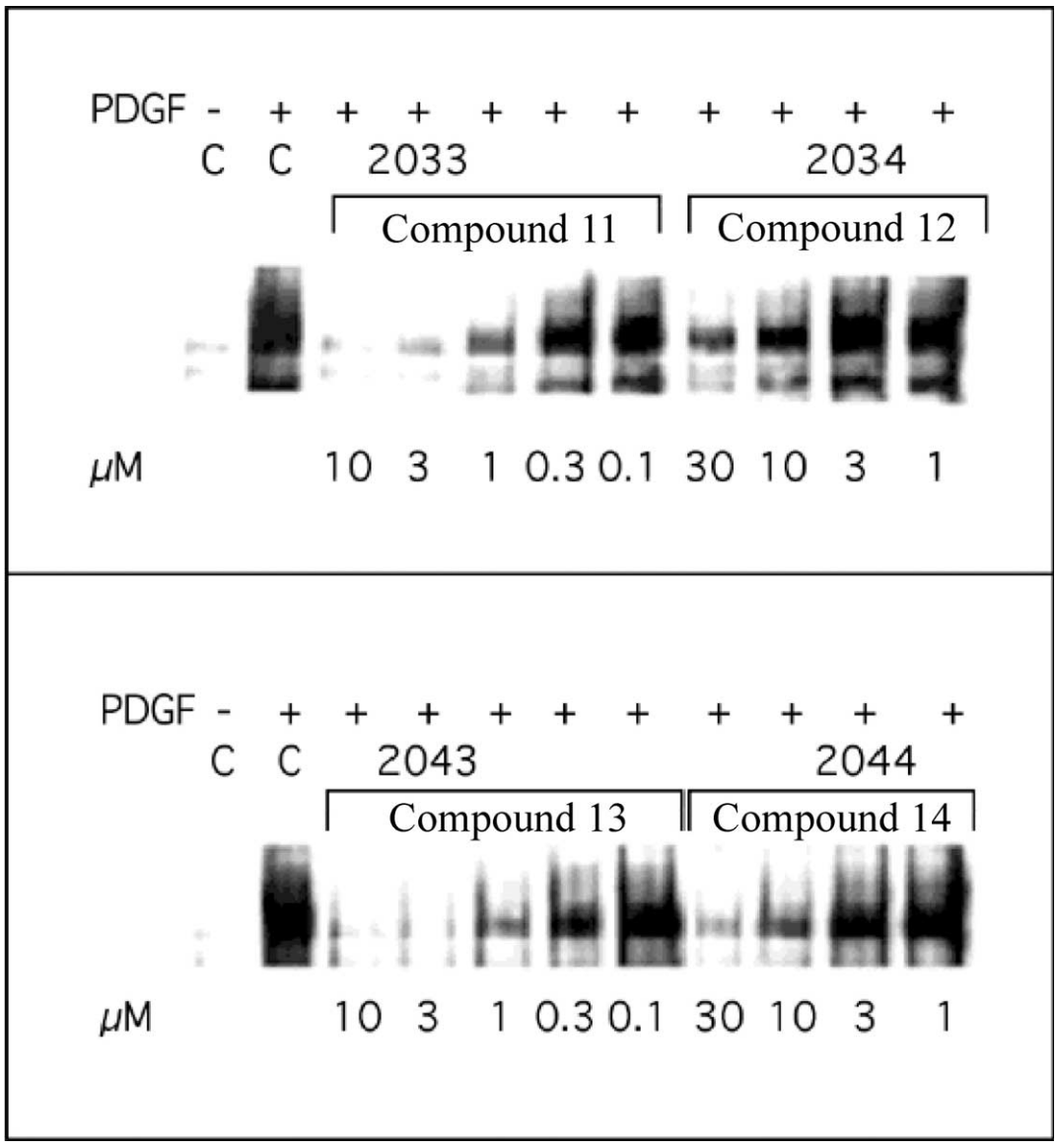

Figure 1. Inhibition of PDGF receptor autophosphorylation by tricyclic quinoxalines. Swiss 3T3 cells were pre-incubated with the indicated concentrations of kinase inhibitors for 2 h before stimulation with PDGF-BB. Cell lysate aliquots were directly subjected to immunoblotting with anti-phosphotyrosine antibodies. Other details are given in the Experimental section. C, control.

diaza and 4 amino or anilide hetero substitution pattern,[14] identical or very similar to adenine. The quinoxalines inhibitors of PDGF receptor possess 1,4 diaza substitution and lack the 4 amino radical and thus are less similar to adenine.[3] Besides the core pharmacophore, all these inhibitors contain an aryl group that interacts with a lipophilic pocket near the ATP binding site, not available to ATP. This extra binding is probably essential to the potency of the inhibitors and seems to be an important factor in their selectivity, as the aryl attachment position is position 3 in the quinoxalines, 4 in quinazolines and 5 in pyrazolo pyrimidines. Thus small differences in the very highly homologous ATP binding sites of tyrosine kinases have made possible the identification of selective inhibitors, a result assumed unlikely a decade ago.[1] Recently, the X-ray study of HCK complexed with PP1[12] and LCK with PP2[13]-shed more light on the exact mode of binding of the pyrazolo pyrimidine to the ATP pocket where the 5-aryl is inserted at lipophilic channel and the 7-*t*-butyl points toward the solvent. For PDGF receptor, neither a three dimensional structure nor a model for the active site have been reported. Therefore, the SAR reported in this study is important for future progress. The transoid configuration (where the aryl and the *N*-methyl are on the opposite side of the molecule) of the higher potency inhibitors compound **11** (AGL 2033) and compound **13** (AGL 2043) bears striking resemblance to the potent tricyclic *N*-methyl pyrrolo quinazoline EGFR kinase inhibitor.[14] While it is tempting to consider that compound **11** (AGL 2033) and compound **13** (AGL 2043) bind to the ATP site with increased affinity, it is also possible that the *N*-methyl in the cisoid conformers compound **12** (AGL 2034) and compound **14** (AGL 2044) causes interference with the pocket wall and thus lowers the affinity of the cisoid isomers. More SAR investigation studies are required to further elucidate the differences between the ATP binding domains of the

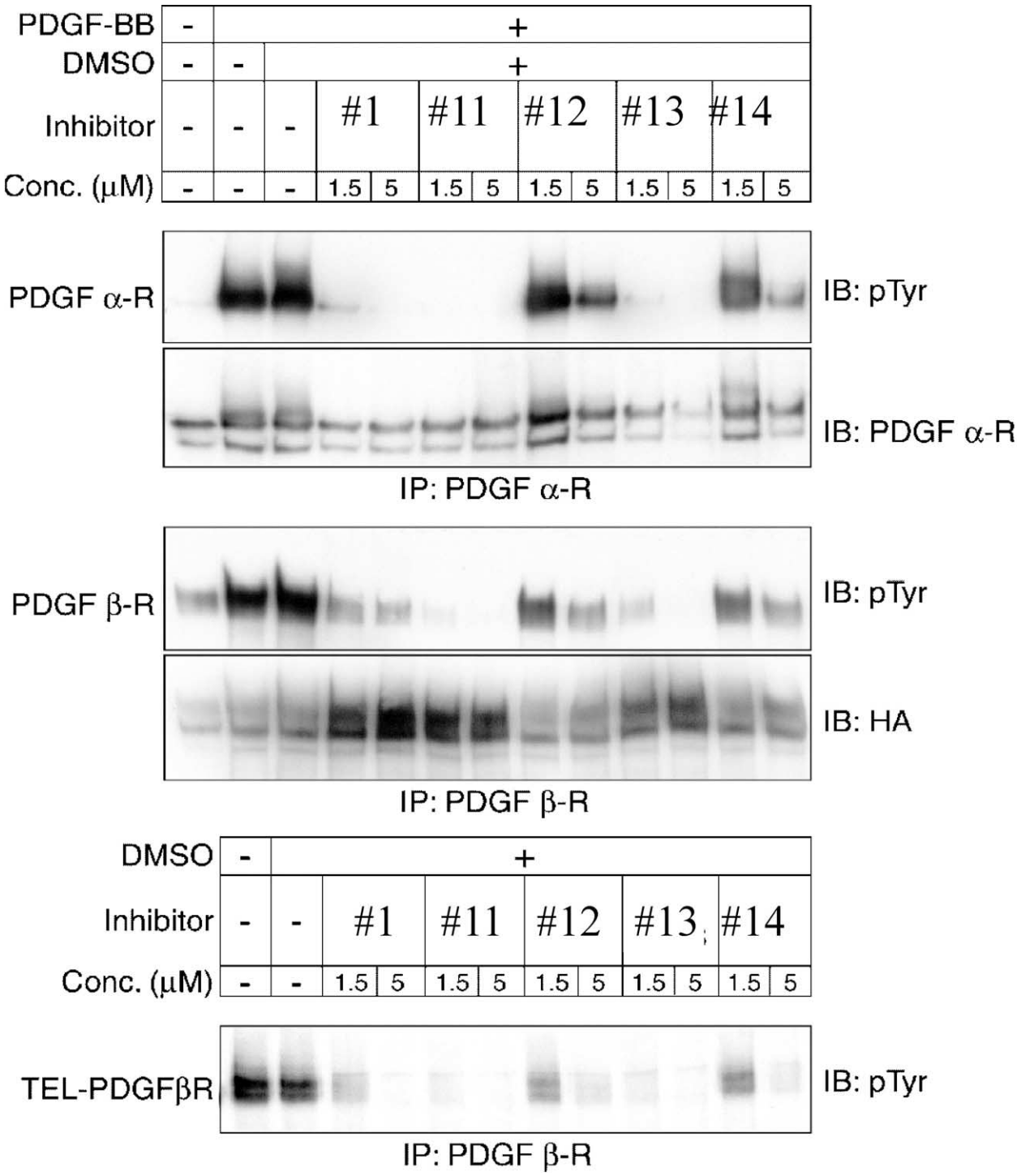

Figure 2. Analysis of tyrphostin activity on BAF3 cells transfected with PDGFR α , β and Tel-PDGFR. PDGFα receptor expressing PAE cells, PDGFβ receptor expressing COS cells and TEL-PDGFβR expressing BAF/3 cells were pre-incubated with the indicated concentrations of kinase inhibitors for 2 h before stimulation with PDGF-BB. Cell lysates were subjected to immunoprecipitation (IP) with PDGF α-receptor or PDGF β-receptor antibody followed by SDS-PAGE in 7% gels. After transfer to PVDF membranes, samples were analyzed by immunoblotting (IB) using phosphotyrosine antibody, PDGF α-receptor antiserum and HA epitope antibody. Experimental details are given in the Experimental protocol.

three classes of PTKs discussed and may allow the construction of a working model for the PDGFR kinase domain. Interestingly compounds **11** and **13** also inhibit more potently the kinase activities of Flt3 and Kit as compared to compounds **12** and **14** (Figs 4 and 5), respectively. This observation conforms to the similarity between the kinase domains of PDGFR, Flt3 and Kit, in the class III of receptor tyrosine kinases.

The improved solubility properties of the tricyclic quinoxalines described here (Table 2) as compared to the bicyclic quinoxalines described by us earlier make them better candidates for clinical development. Indeed, preliminary experiments suggest that compound **13** (AGL 2043) is highly effective in the inhibition stenosis in the pig heart subsequent to balloon-induced injury (work in progress). Additionally, compound **13** potently inhibits the

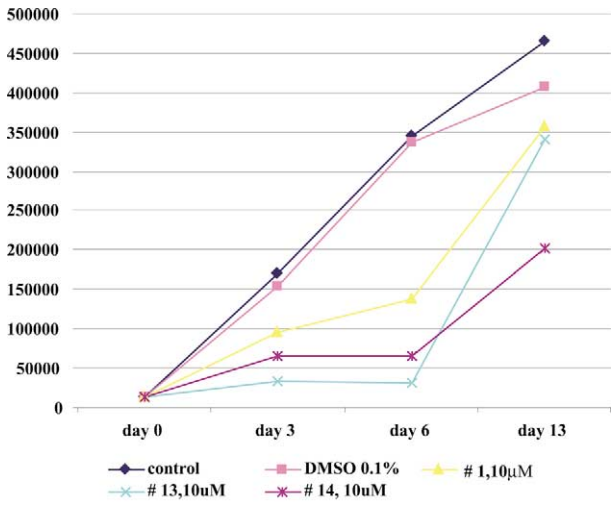

Figure 3. Inhibitory action of compounds **13** (AGL 2043) and **14** (AGL 2044) on the proliferation of pig heart smooth muscle cells. Smooth muscle cells were prepared as described by us earlier.[7] Drug was removed on day 6.[7]

proliferation of leukemic blasts harboring FLT3 mutations (data not shown), a notable observation since mutations of FLT3 are the most common molecular abnormalities described in acute myelogenous leukemia to date.[10]

The cytostatic actions of the compounds compound **11** (AGL 2033); compound **13** (AGL 2043) (Fig. 3) and compound **1**[7] on smooth muscle cells are fully reversible. Also, growth inhibition of FLT3 or KIT driven cells by these quinoxalines can be reversed by withdrawal of the agents (data not shown). This feature suggests that these compounds are non-toxic and may be considered as good candidates for development as anti-restenosis agents. These compounds are also possible candidates for the treatment of malignancies driven by PDGFR, Tel-PDGFR, FLT3, or KIT.

Conclusion

Here, we describe imidazolo quinoxalines, which are potent and selective class III tyrosine kinase inhibitors. These compounds posses balanced solubility properties and seem to be non-cytotoxic. Therefore, they are more suitable than the highly hydrophobic bicyclic quinoxalines for development as anti-cancer and anti-restenosis agents.

Experimental

Materials and methods

All starting materials were purchased from Aldrich. NMR spectra were recorded on a Bruker AMX-300 pulsed FT spectrometer. Chemical shifts are in ppm

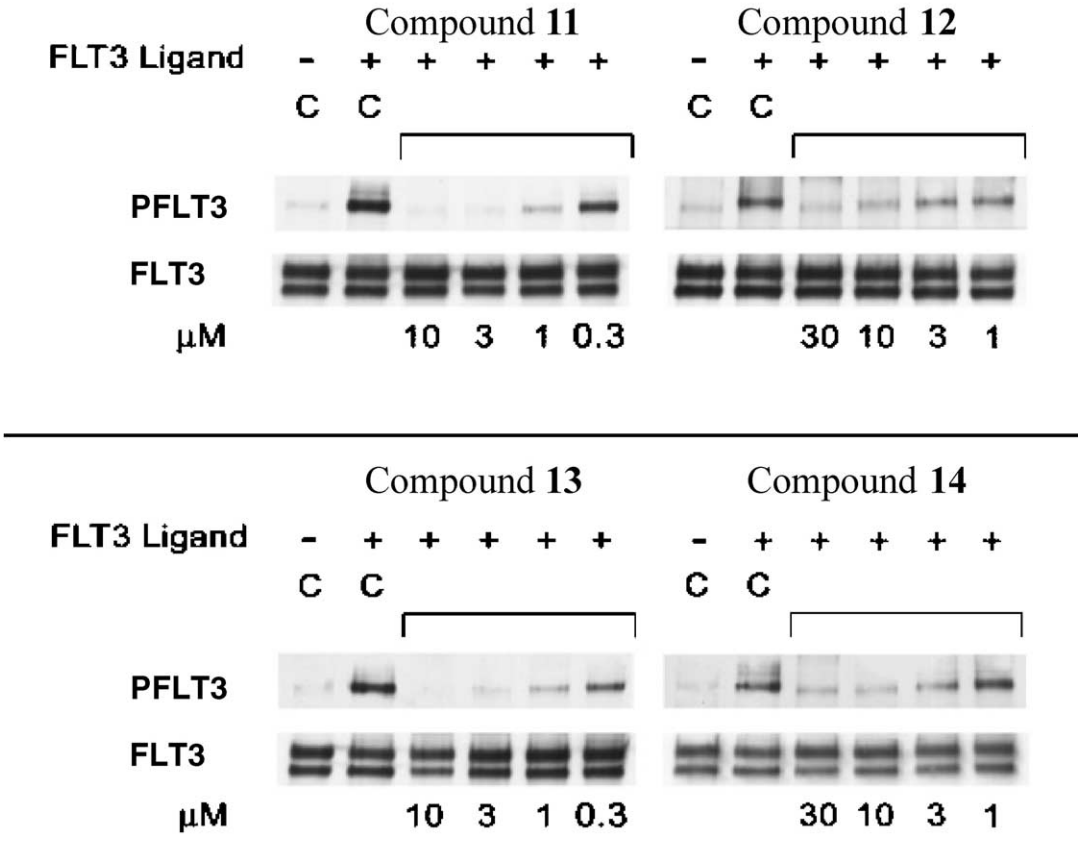

Figure 4. Analysis of tyrphostin activity on BAF/3 cells transfected with FLT3. BAF/3 cells were pre-incubated with the indicated concentrations of kinase inhibitors for 2 h before stimulation with FLT3 ligand. Cell lysates were subjected to immunoprecipitation (IP) with FLT3 antibody followed by SDS-PAGE in 10% gels. After transfer to nitrocellulose membranes, samples were analyzed by immunoblotting (IB) using phospho-FLT3 antibody and FLT3 antibody. Other details are given in the Experimental Section. C, Control.

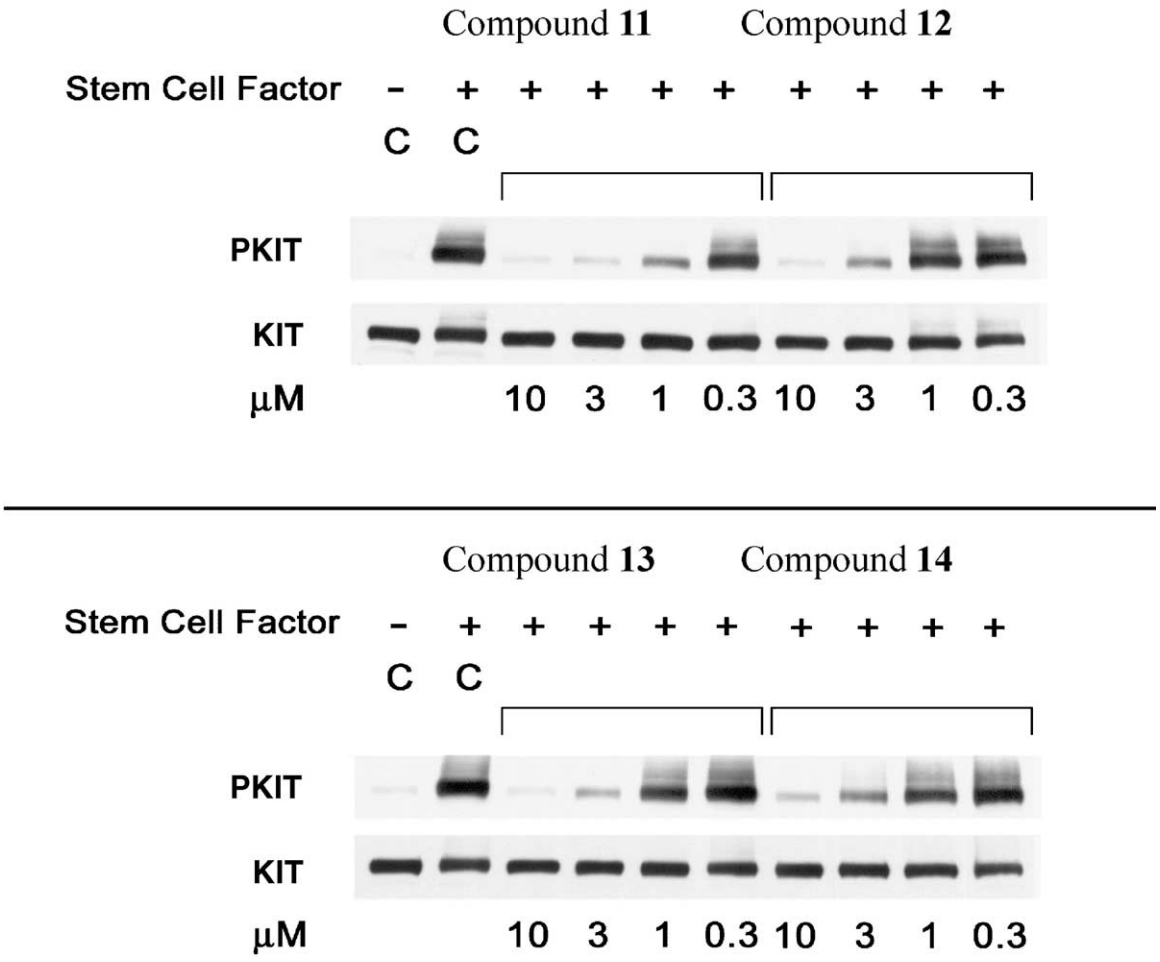

Figure 5. Analysis of tyrphostin activity on MO7e cells expressing KIT receptor. MO7e cells were pre-incubated with the indicated concentrations of kinase inhibitors for 2 h before stimulation with KIT ligand (stem cell factor). Cell lysates were subjected to SDS-PAGE in 10% gels. After transfer to nitrocellulose membranes, samples were analyzed by immunoblotting (IB) using phospho-KIT antibody and KIT antibody. Experimental details are given in the Experimental protocol.

relative to the TMS internal standard. Mass spectra were recorded with a Finnigan Mat 4600 instrument.

Combustion analyses for all new compounds were within 0.4% of theoretical values. Microanalyses were performed by the Hebrew University Analytical Services and are reported in Supporting Information.

X-ray crystal structure determination

Data were collected on an ENRAF-NONIUS CAD-4 computer controlled diffractometer. CuK_α, ($\lambda = 1.54178$ Å). Irradiation was performed with a graphite crystal monochromator in the incident beam. The unit cell dimensions were obtained by a least squares fit of 20 centered reflections in the $23° < \theta < 127°$ range. Intensity data were measured by using the ω-2θ technique to a maximum 2θ of 120°. The scan width, $\Delta\omega$, for each reflection was $0.8 \pm 0.15 \tan\theta$ with a scan time of 20 s. Background measurements were made at both limits of each scan. Three standard reflections were monitored every 60 min. No systematic variations in intensities were noticed.

Intensities were corrected for Lorentz and polarization effects. All non-hydrogen atoms were found by using the results of a MULTAN direct method analysis. After several cycles of refinement (All crystallographic computing was done on a VAX 9000 computer at the Hebrew University of Jerusalem, using the TEXSAN structure determination software). The positions of the hydrogen atoms were calculated and introduced with a constant isotropic temperature factor of 0.5 A^2. Refinement proceeded to convergence by minimizing the function $\Sigma\omega(|F_0| - |F_c|)^2$, where the weight ω is $\sigma(F_0)^{-2}$. The discrepancy indices $R = \Sigma(|F_0| - |F_c|)/\Sigma|F_0|$ and $R_w = [\Sigma\omega(|F_0| - |F_c|)^2/\Sigma\omega(|F_0|)^2]^{1/2}$ are available upon request.

Synthetic methods

The structures of the compounds synthesized are presented in the Results section.

2-Methyl benzimidazole (4). 32 g phenylene diamine and 60 mL acetic acid were refluxed for 2 h. Ice and KOH were added to pH = 8 and the light violet solid filtered

out. Recrystalization from benzene gave 30 g light yellow solid, mp 170 °C, 77% yield. NMR $CDCl_3$ δ 7.23 (4H, m), 2.64 (3H,s).

1,2-Dimethyl benzimidazole (5). 15 g, 105 mmol, methyl iodide was added to 10 g, 75 mmol, **4** and 25 g, 450 mmol, crushed KOH in 300 mL acetone at room temperature during 0.5-h period. 0.5 h later water was added and the reaction was extracted with CH_2Cl_2, evaporated and chromatographed on silica gel to produce 6 g, 54% yield, white solid, mp 102 °C[15] (mp 111 °C). NMR $CDCl_3$ δ 7.68 (1H, m), 7.25 (3H, m), 3.72 (3H, s, *N*-methyl), 2.64 (3H, s).

1,2-Dimethyl 5,6-dinitro benzimidazole (9). 3.3 g **5** in 15 mL HNO_3 (70%) was cooled with ice and 10 mL concd sulphuric acid was added slowly. The reaction was then stirred at 100 °C for 2 h, poured on ice and neutralized with KOH. Filtering gave 4 g, 93% yield, of pale blue-white solid. The solid consists of ~80% 1:1 mixture of **6**,5-nitro: **7**,6-nitro. ~10% **8**,4-nitro and10%, **9** 5,6-dinitro isomers.

6, 5-Nitro. NMR $CDCl_3$ δ 8.52 (1H, d, $J=2$ Hz, H_4), 8.16 (1H, dd. $J=8.8$, 2.0 Hz, H_6). 7.69 (1H, d, $J=8.8$ Hz, H7), 3.81 (3H,s), 2.66 (3H,s). NMR acetone-d_6 δ 8.40 (1H, d, $J=2$ Hz, H_4), 8.16 (1H, dd, $J=8.8$, 2.0 Hz, H_6). 7.66 (1H, d, $J=8.8$ Hz, H7), 3.96 (3H,s), 2.65 (3H,s).

7, 6-Nitro. NMR $CDCl_3$ δ 8.22 (1H, d, $J=2$ Hz, H_7), 8.12 (1H, dd, $J=8.8$, 2.0 Hz, H_5). 7.31 (1H, d, $J=8.8$ Hz, H4), 3.78 (3H,s), 2.64 (3H,s). NMR acetone-d_6 δ 8.38 (1H, d, $J=2$ Hz, H_4), 8.10 (1H, dd. $J=8.8$, 2.0 Hz, H_6). 7.62 (1H, d, $J=8.8$ Hz, H7), 3.90 (3H,s), 2.63 (3H,s). These assignments are not certain and may be reversed.

MS mixture of 5- and 6-nitro isomers. 191 (M^+, 100%), 161 (M−NO, 51%), 145 (M−NO_2, 28), 133 (25), 130 (M−NO_2−CH_3, 23), 104 (22), 63 (28) *m*/*e*.

8, 4-Nitro or 7-nitro. NMR $CDCl_3$ δ 9.03 (1H, d), 8.80 (1H, q), 8.54 (1H, d), 3.94 (3H, s), 2.74 (3H, s). B.1.5 g mixture from A was treated with 10 mL HNO_3 (70%) and 6 mL concd sulphuric acid at 190 °C for 3.5 h, poured on ice and neutralized with KOH. Filtering produced light green solid. Recrystalization from ethanol gave 0.48 g, 26% yield, white solid, mp 224 °C, pure 5,6-dinitro isomer **9**. NMR $CDCl_3$ δ 8.17 (1H, s), 7.90 (1H, s), 3.87 (3H, s), 2.73 (3H, s). NMR acetone-d_6 δ 8.31 (1H, s), 8.22 (1H, s), 4.03 (3H, s), 2.75 (3H, s).

The nitration reaction seems to be sensitive to the ratio of acids as well as reaction temperature and time. Thus the reaction as in B at 160 °C for 1.5 h produced 15% 5,6-dinitro isomer **9**. While the reaction with solid KNO_3 and concentrated sulphuric acid at room temperature produced between 15 and 60% of the 5,6-dinitro isomer.

1,2-Dimethyl 3,6-diaminobenzimidazole (10). 0.7 g of pure 5,6-dinitro isomer **9** and 0.2 g of Pd/C in 20 mL ethanol and 20 mL acetic acid were hydrogenated for 4 h. Filtering and evaporating produced 0.5 g, 95% yield, white solid, mp 212 °C.

Compounds 11 and 12. 0.5 g, 2.8 mmol, **10** and 0.45 g, 3 mmol, phenyl glyoxal hydrate in 20 mL ethanol and 20 mL acetic acid were refluxed for 3 h, neutralized with NaOH, extracted with CH_2Cl_2, evaporated and chromatograohed on silica gel. The more active inhibitor, isomer **11**, moves a little faster on silica gel plate. $R_f=0.6$ (5:95 CH_3OH/CH_2Cl_2) while isomer **12** has $R_f=0.5$.

Chromatography on 150 g silica gel, 70–230 mesh, eluting with 1% methanol in CH_2Cl_2 produced as follows.

1,2-Dimethyl-6-phenyl imidazolo [5,4-*g*] quinoxaline (11). From first fractions: 0.265 g, 32% yield, light yellow solid, mp 275 °C d. NMR $CDCl_3$ δ 9.30 (1H, s, H7), 8.45 (1H, s, H4), 8.21 (2H, m), 7.95 (1H, s, H9), 7.50 (3H, m), 3.88 (3H, s, *N*-methyl), 2.75 (3H, s, 2-methyl). High-resolution MS (CI) *m*/*e* (calcd 274.121847) −274.121445 (M^+, 100%), 259.096 (M-CH_3, 5%), 230.985 (M−N−CH_3, 25%), 196.98 (M−Ph, 5), 163.011 (6), 149.025 (12), 144.067 (M−Ph−HCN−CN, 11), 130.992 (25).

1,2-Dimethyl-7-phenyl imidazolo [5,4-*g*] quinoxaline (12). From the following fractions: 0.265 g, 32% yield, light yellow solid mp 218 °C. NMR $CDCl_3$ δ 9.32 (1H, s, H7), 8.42 (1H, s. H4), 8.21 (2H, m), 8.0 (1H, s, H9), 7.50 (3H, m), 3.88 (3H, s, *N*-methyl), 2.75 (3H, s, 2-methyl).

The assignment of structure to compounds **11** and **12** is only tentative. In analogy to compounds **13** and **14**, the TLC mobilities, the small difference in NMR spectra between the compounds as well as the differences in biological efficacies suggest that compound **11** has the transoid configuration. The final determination awaits X-ray analysis, similar to that performed on **13** and **14**.

Compound 22. Compound 21. 7 g, 55 mmol, 2-acetyl thiophene, 14 g, 55 mmol, Iodine and 12 mL pyridine in 100 mL ethanol were refluxed for 2.5 h. After standing at room temperature for 1 h it was filtered, washed with ethanol and dried to give 13.7 g yellow green solid, which was a 1:1 mixture with pyridinium iodide. The yield for 6.85 g was 38%. The reaction of 42 g of acetyl thiophene produced 104 g solid, 47% yield. NMR DMSO-d_6 8.55 (2H, d, $J=5.5$ Hz), 8.49 (2H, d, $J=5.0$ Hz), 8.27 (1H, t, $J=7.8$ Hz), 8.07(1H, t, $J=7.8$ Hz), 7.71 (4H, m), 7.55 (2H, t), 6.96 (1H, dd (t)), 5.93 (2H,s).

2′-Pyridinium iodide-2-acetyl thiophene (22). 9.9 g, 30 mmol, **20** and 5.3 g, 35 mmol, *p*-dimethyl amino nitrosobenzene in 100 mL ethanol were cooled with ice and 21 g, 52 mmol, NaOH in 100 mL water was added. After 2 h of cooling, the reaction was extracted with CH_2Cl_2, evaporated and chromatographed on silica gel (elution with CH_2Cl_2) to give 0.35 g, 8% yield, red-brown solid, a 60:40 *syn*/*anti* mixture by NMR.

Following chromatography, the reaction of 104 g **21** produced 11.7 g red solid, yield from acetyl thiophene 13%.[16] NMR $CDCl_3$ δ 60:40 *syn*/*anti* mixture from 3.06:2.97 ppm 60:40. 8.46 (d), 8.36 (d), 8.27 (vinyl, s), 7.84 (d), 7.72 (d), 7.24 (m), 7.58, 7.22 (ABq, anti), 7.48, 6.74 (ABq, *syn* 60%).

NOTE: The nitrone **22** can be hydrolyzed with HCl to give thiophene glyoxal 23 which can be used to react with the diamine **10**, but in the synthesis of compound **13** it was generated in situ.

Compounds 13 and 14. 4.6 g, 20 mmol, 5,6-dinitro **10** and 0.6 g 5% Pd/C in 30 mL ethanol and 30 mL acetic acid were hydrogenated for 4 h. After filtering 6.3 g, 23 mmol, nitrone **22** and 1 mL HCl were added and the reaction was refluxed for 1.5 h. It was neutralized with KOH, extracted with CH_2Cl_2 and evaporated.

Chromatography on 200 g silica gel, 70–230 mesh, eluting with 1% methanol in CH_2Cl_2 produced as follows.

1,2-Dimethyl-6-(2-thiophene) imidazolo [5,4-*g*] quinoxaline (13). First fractions gave 0.23 g, 4% yield, light yellow solid, and mp 274 °C. R_f = 0.6 (5:95 CH_3OH/CH_2Cl_2). NMR $CDCl_3$ δ 9.20 (1H, s, H7), 8.34 (1H, s. H4), 7.87 (1H, s, H9), 7.83, 7.52, 7.20 (3H.ABX 12 line m, thiophene), 3.88(3H, s, *N*-methyl), 2.75 (3H, s, 2-methyl). Assignment of H4 and H_9 is not certain and may be reversed. Spectra of **13** and **14** were recorded separately and looked identical. When a sample of two pure isomers was mixed and recorded all signals overlapped except two singlets at 9.22 ppm and 7.90, 7.88 ppm.

NMR acetone-d_6 δ 9.38 (1H, s, H7), 8.12 (1H, s, H4), 8.02 (1H, s, H9), 8.08, 7.71, 7.27 (3H.ABX 12 line m, thiophene), 3.97 (3H, s, *N*-methyl), 2.70 (3H, s, 2-methyl).

Note that H_4 and H_9 do not overlap.

NMR DMSO-d_6 δ 9.48 (1H, s, H7), 8.15 (1H, s, H4), 8.09 (1H, s, H9), 8.18, 7.81, 7.28 (3H.ABX 12 line m, thiophene), 3.88 (3H, s, *N*-methyl), 2.66 (3H, s, 2-methyl).

NMR nitrobenzened$_5$ 9.0(1H, s, H7), 8.01 (1H, s. H4), 7.60 (1H, s, H9), 7.61, 7.27, 6.92 (3H.ABX 12 line m, thiophene), 3.50 (3H, s, N–CH_3), 2.38 (3H, s, 2-CH_3).

High-resolution MS (CI) *m*/*e* (calcd 280.078268) −280.07560 (M^+, 100%), 242.15 (14%), 230.985 (10), 168.989 (30), 140.037 (7), 130.992 (17), 118.992 (18).

MS *m*/*e* (AG 1992-mixture of 2043, 2044)-280 (M^+, 100%), 253 (M−HCN, 8%), 144 (M−thiophene−HCN−CN, 48%), 127 (13), 111 (11), 88 (14), 76 (9).

The purity of compound **13** (AGL 2043) was 97.1%. R_f = 0.5 in HPLC acetonitrile–water gradient, RP-18, R_t = 11.9 min. Elementary analysis C = 64.01, H = 4.26, N = 20.15.

1,2-Dimethyl-7- (2-thiophene) imidazolo [5,4-*g*] quinoxaline (14). Following fractions gave 0.6 g, 11% yield, light yellow solid, mp 218 °C. R_f = 0.5 (5:95 CH_3OH/CH_2Cl_2). nMR $CDCl_3$ δ 9.22 (1H, s, H_6), 8.34 (1H, S, H_4), 7.90 (1H, s, H_9), 7.83, 7.52, 7.20 (3H.ABX 12 line m, thiophene), 3.88 (3H, s, *N*-methyl), 2.75 (3H, s, 2-methyl). NMR acetone-d_6 δ 9.38 (1H, s, H_7), 8.15 (1H, s, H_4), 7.96 (1H, s, H_9), 8.08, 7.71, 7.27 (3H.ABX 12 line m, thiophene), 3.97 (3H, s, *N*-methyl), 2.70 (3H, s, 2-methyl). NMR DMSO-d_6 δ 9.46 (1H, s, H_7), 8.14 (1H, s, H_4),8.13 (1H, s, H_9),8.18, 7.81, 7.28 (3H.ABX 12 line m, thiophene), 3.88 (3H, s, *N*-methyl), 2.66 (3H, s, 2-methyl). NMR nitrobenzene-d_5 9.0 (1H, s, H_7), 8.05 (1H, s, H_4), 7.47 (1H, s, H_9), 7.64, 7.32, 6.95 (3H.ABX 12 line m, thiophene), 3.50 (3H, s, *N*-methyl), 2.38 (3H, s, 2-methyl).

The X-ray of crystals grown from CH_3CN solutions shows the higher R_f, more active isomer is **13**, with the *transoid* 1-methyl-thiophene configuration while **14**, has the *cisoid* configuration (transoid and *cisoid* denote the relation of the pharmacophore; cis and trans notations are reserved for configuration about double bonds).

2-Chloroacetyl ferrocenne (15). To 5.5 g, 30 mmol, ferrocenne and 3.4 g, 30 mmol, chloro acetyl chloride in 60 mL CH_2Cl_2 was added 4.2 g, 31 mmol, $AlCl_3$. After 2 h at room temperature, 5 mL HCl was added and the blue-black reaction was worked up. Chromatography gave 350 mg, 5% yield, red solid. NMR $CDCl_3$ δ 4.86 (2H, t, J = 1.8 Hz), 4.62 (2H, t, J = 1.8 Hz), 4.43 (2H, s), 4.27 (5H, s).

3-Ferrocenne 6,7-dimethyl quinoxaline (17). 150 mg, 0.6 mmol, **15** and 80 mg, 0.6 mmol, 4,5-dimethyl phenylene diamine in 4 mL DMSO were heated for 2 h at 100 °C. Workup (KOH, CH_2Cl_2), chromtography and trituration with hexane yielded 10 mg red solid, 5% yield. NMR $CDCl_3$ δ 8.88 (1H, s), 7.78 (1H, s), 7.77 (1H, s), 5.09 (2H, t, J = 1.8 Hz), 4.53 (2H, t,J = 1.8 Hz),4.08 (5H, s), 2.49 (3H, s), 2.47 (3H, s).

1,2-Dimethyl 6-ferrocene imidazolo[5,4-*g*] quinoxaline (18). 80 mg, 0.45 mmol, **10** and 130 mg, 0.5 mmol, **15** in 4 mL DMSO were heated 2 h at 100 °C. Workup (KOH, CH_2Cl_2), chromatography and trituration with hexane yielded 15 mg red solid, 9% yield. NMR $CDCl_3$ δ 8.96 (1H, s), 8.30, 8.28 (1H, 2s), 7.96 (1H, s), 5.13 (2H, t, J = 1.8 Hz), 4.55 (2H, t, J = 1.8 Hz), 4.11 (5H, s), 3.86 (3H, s), 2.71 (3H, s).

Compound **18** is probably mixture of cisoid and transoid isomers whose NMR spectra overlaps except at 8.30, 8.28 ppm.

MS *m*/*e* 383 (M^+, 100%).

2-Thiophene 6,7-dimethyl quinoxaline (19). 400 mg, 1.5 mmol, thiophene nitrone 21 and 230 mg, 1.7 mmol, 4,5-dimethyl phenylene diamine in 30 mL ethanol and 0.3 mL HCl were heated for 2 h at 100 °C. Workup (KOH, CH_2Cl_2), chromatography and trituration with hexane

yielded 180 mg yellow solid, 50% yield, mp 151 °C. NMR $CDCl_3$ δ 9.13 (1H, s), 7.81 (2H, s), 7.83, 7.50, 7.19 (12 line ABX m), 2.49 (6H, s), 2.47 (3H, s). MS *m/e* 240 (M^+, 100%), 225 (M−methyl, 12%), 213 (M−HCN, 9),198 (M−methyl−HCN, 8), 130 (M−thiophene−HCN, 5), 103 (12), 77 (10).

Inhibition of PDGFR kinase activity

Swiss 3T3 fibroblasts (ATCC CCL 92) were cultivated in DMEM/10% FCS (Life Technologies). The effect on PDGF-stimulated tyrosine phosphorylation was measured by subjecting quiescent cultures in 24-well plates (NUNC) to a medium change into serum-free DMEM (0.4 mL per well) and treating them with the test compounds in DMSO (final DMSO concentration 1%) or solvent for 2 h. The cells were subsequently stimulated with 100 ng/mL human recombinant PDGF-ββ (TEBU/Peprotech) or mock-treated for 10 min at room temperature, washed twice with PBS and extracted with lysis buffer containing Hepes, pH 7.5, 1% Triton X-100, phosphatase and protease inhibitors as described.[3] 10 μg protein of cell extracts were subjected to SDS-PAGE with 7.5% gels and immunoblotting with anti-phosphotyrosine antibodies. Quantification of IC_{50} values was based on the intensity of the signal for autophosphorylated PDGF receptor. Titration was performed using 4–8 inhibitor concentrations within a range of two orders of magnitude, which was selected on the basis of preliminary experiments. Results were subjected to curve fitting using the program Sigma Plot 2.0 (Jandel Corporation). Purification of human PDGFβ-receptor and in vitro kinase reactions with purified receptor were performed as described earlier.[3,5,6] To measure effects on EGF receptor phosphorylation, A431 cells (ATCC CRL 1555) were starved overnight in serum-free medium, treated for 2 h with the compounds, thereafter stimulated with 100 ng/mL EGF (TEBU/Peprotech) for 10 min and subjected to extraction and immunoblotting as described above. Src-dependent tyrosine phosphorylation in src-transformed NIH-fibroblasts was determined as described.[5]

Activity on Src kinase, IGF-1R and EGFR, pp60c-Src, PKA and PKB In cell-free assays

The general tyrosine kinase substrate poly (Glu, Tyr) 4:1, (PGT), (Sigma), was coated onto 96-well Maxisorp plates (Nunc) by adding 125 μL 0.1 mg/mL PGT in phosphate-buffered saline to each well. Plates were sealed and incubated for 16 h in 37 °C, washed once with TBST (10 mM Tris–HCl pH 7.5, 50 mM NaCl and 0.1% Triton X-100), dried for 2–3 h at 37 °C and stored at 4 °C.

50 ng of purified GST-Src[17] per well were incubated in 20 mM Tris–HCl pH 7.5, 10 mM $MgCl_2$ with or without inhibitors for 20 min at 30 °C.

Phosphorylation of tyrosyl residues was initiated by the addition of 20 μM ATP and terminated 10 min later by the addition of EDTA to a final concentration of 200 mM. Plates were washed five times with TBST and blocked with 5% low-fat (1%) milk. For quantification of phosphorylated tyrosines, plates were incubated with rabbit polyclonal anti-phosphotyrosine serum for 1 h at room temperature, washed five times, and incubated with anti-rabbit peroxidase-conjugated antibody for 45 min.

Detection was carried out using a color reagent, 2,2′-azido-bis 3-ethylbenzihiazoline-6-sulfonic acid (ABTS) (Sigma) in citrate–phosphate buffer pH 4 with 0.004% H_2O_2 for 10 min and monitored at OD 405 nm.

IC_{50} values of inhibitors were determined using the REGRESSION program. (Blackwell Scientific Software, Osney Mead, Oxford, UK). Activity of EGFR,[18] IGF1-R[19] and Insulin receptor[19] kinase were measured as described PKB/Akt activity and PKA activity were measure as described.[20]

BAF/3 Wild Type FLT3 stable constructs

Human FLT3 cDNA generously provided by Dr. Rosnet (Molecular Oncology Unit, INSERM) was expressed in a pLXSN Retroviral Vector (Clontech). The vector containing FLT3 was transfected into a 1:1 mix of EcoPack and AmphoPack 293 packaging cells (Clontech) using Lipofectamine and PLUS reagent (Invitrogen). Supernatant from these packaging cells was filter sterilized, supplemented with 5 ng/mL murine IL-3, and used to transduce BAF/3 cells. BAF/3 cells were primarily selected using 1100 ng/mL Geneticin (G418 Sigma) and then secondarily selected using 5 ng/mL recombinant human FLT3 ligand (R&D) in the absence of murine IL-3.

Analysis of tyrphostin activity on BAF/3 cells transfected with PDGFR α, β, Tel-PDGFR or FLT3, Mo7e and COS/PDGFRβ

The tyrphostins compounds **2**, **11**, **12**, **13** and **14** were prepared as stock solutions of 10 mM in DMSO. Porcine aortic endothelial (PAE) cells stably expressing the human PDGFα-receptor,[21] BAF/3 cells stably expressing the TEL-PDGFβ R fusion protein,[22] BAF/3 cells stably expressing human FLT3, MO7e cells with naturally occurring KIT receptor, or COS cells transiently transfected with a plasmid encoding the human PDGF β-receptor[23] using the calcium phosphate protocol, were starved overnight in a culture medium containing 0.1% fetal calf serum. Following a 2-h incubation with tyrphostins or vehicle control in serum-free media, cells were washed once in ice-cold phosphate-buffered saline (PBS) with 0.1% bovine serum albumin (BSA) and stimulated with 50 ng/mL PDGF-ββ for 1 h at 4 °C, 100 ng/mL FLT3 ligand, 100 ng/mL KIT ligand (human stem cell factor), followed by a rinse in ice-cold PBS. After extraction with lysis buffer (20 mM Tris–HCl pH 7.5, 150 mM NaCl, 0.5% Triton X-100, 0.5% deoxycholic acid, 10 mM EDTA, 1 mM phenylmethylsulfonyl fluoride, 1% aprotinin, 200 mM Na_3VO_4) and centrifugation at 10,000*g* for 15 min, immunoprecipitation was performed using the PDGFα-receptor antiserum R7[20] or PDGFβ-receptor antiserum R3,[23] or FLT3 antiserum for 60 min at 4 °C. Following incubation with Protein A Sepharose 6MB (Amersham Pharmacia Biotech) for 30 min at 4 °C,

samples were washed three times in lysis buffer and heated for 5 min at 95 °C. The immunoprecipitation step was not required for the lysates of the MO7e cells.

After SDS-PAGE in 7% gels and semi-dry transfer onto polyvinylidene difluoride (PVDF) membranes [PDGFR] or 10% gels in wet transfer to nitrocellulose [FLT-3 and KIT], the filters were blocked in TBS/0.1% Tween-20. Immunoblotting was performed using the phosphotyrosine antibody PY20 (Transduction Laboratories), phospho-FLT3 (Cell Signaling), or phospho KIT (Cell Signaling). After stripping, the filters were reprobed with PDGF-α-receptor antiserum R7, HA epitope antibody (Boehringer Mannheim), S-18 FLT3 antibody (Santa Cruz Biotechnology), or KIT antibody (Oncogene). Protein bands were visualized using enhanced chemiluminiscense (ECL, Amersham Pharmacia Biotech).

Action of tyrphostins on aorta smooth muscle cells

The effect of the tyrphostins was examined on smooth muscle cells from abdominal pig aortas, as described earlier.[7] It can be seen that compounds **13** (AGL 2043) and **14** (AGL 2044) are superior to compound **1** (AG1295). Tyrphostin (10 μM) were added to the cells and reached 10,000 cells per well. The compound was washed out on day 6. It can be seen that the action of all three tyrphostins is reversible.

Acknowledgements

Supported in part by a Infrastructure grant from the Ministry of Science in Jerusalem, Israel to A.L., in part from the Minfunding, from a VA Merit Review Grant (M.C.H.) and the Doris Duke Charitable Foundation (M.C.H. and K.Y) and in part by the Deutsche Forschungsgemeinschaft: Wa734/4-2 and the Heisenberg Scholarship to J.W.

References and Notes

1. Levitzki, A. *Pharmacol. Ther*. **1999**, *82*, 231.
2. Gazit, A.; App, H.; McMahon, G.; Chen, J.; Levitzki, A.; Böhmer, F. D. *J. Med. Chem*. **1996**, *39*, 2170.
3. Kovalenko, M.; Gazit, A.; Böhmer, A.; Rorsman, C.; Ronnstrand, L.; Heldin, C. H.; Waltenberger, J.; Böhmer, F. D.; Levitzki, A. *Cancer Res*. **1994**, *54*, 6106.
4. Lipson, K. E.; Pang, L.; Huber, L. J.; Chen, C.; Tsai, J. M.; Hirth, P.; Gazit, A.; Levitzki, A.; McMahon, J. *J. Pharm. Exp. Therapeutics* **1998**, *285*, 844.
5. Waltenberger, J.; Uecker, A.; Kroll, J.; Frank, H.; Mayr, U.; Bjorge, J. D.; Fujita, D.; Gazit, A.; Hombach, V.; Levitzki, A.; Böhmer, F. D. *Circulation Res*. **1999**, *85*, 12.
6. Kovalenko, M.; Ronnstrand, L.; Heldin, C. H.; Loubtchenkov, M.; Gazit, A.; Levitzki, A.; Böhmer, F. D. *Biochemistry* **1997**, *36*, 6260.
7. Banai, S.; Wolf, Y.; Golomb, G.; Pearle, A.; Waltenberger, J.; Fishbein, I.; Schneider, A.; Gazit, A.; Perez, L.; Huber, R.; Lazarovichi, G.; Rabinovich, L.; Levitzki, A.; Gertz, D. *Circulation* **1998**, *97*, 1960.
8. Karck, M.; Meliss, M. R.; Hestermann, M.; Mengel, M.; Pethig, K.; Levitzki, A.; Banai, S.; Golomb, G.; Fishbein, I.; Chorny, M.; Haverich, A. *Transplantation* **2002**, *74*, 1335.
9. George, D. *Semin. Oncol*. **2001**, *5* (Suppl. 17), 27.
10. Gilliland, D. G.; Griffin, J. D. *Blood* **2002**, *100*, 1532.
11. Heinrich, M. C.; Rubin, B. P.; Longley, B. J.; Fletcher, J. A. *Hum. Pathol*. **2002**, *33*, 484.
12. Schindler, T.; Sicheri, F.; Pico, A.; Gazit, A.; Levitzki, A.; Kuriyan, J. *Mol. Cell* **1999**, *3*, 639.
13. Zhu, X.; Kim, J. L.; Newcomb, J. R.; Rose, P. E.; Stover, D. R.; Toledo, L. M.; Zhao, H.; Morgenstern, K. A. *Struct. Fold Des*. **1999**, *7*, 651.
14. Traxler, P.; Green, J.; Mett, H.; Sequin, U.; Furet, P. *J. Med. Chem*. **1999**, *42*, 1018.
15. Kikugawa, Y. *Synthesis* **1981**, *3*, 124.
16. Kronke, F.; Borner, E. *Berichte* **1936**, *69*, 2006.
17. Karni, R.; Mizrachi, S.; Reiss-Sklan, E.; Gazit, A.; Livnah, O.; Levitzki, A. *FEBS Lett*. **2003**, in press.
18. Ortu, G.; Ben-David, I.; Rozen, Y.; Freedman, N. M.; Chisin, R.; Levitzki, A.; Mishani, E. *Int. J. Cancer* **2002**, *101*, 360.
19. Blum, G.; Gazit, A.; Levitzki, A. *Biochemistry* **2000**, *39*, 15705.
20. Reuveni, H.; Livnah, N.; Geiger, T.; Klein, S.; Ohne, O.; Cohen, I.; Benhar, M.; Gellerman, G.; Levitzki, A. *Biochemistry* **2002**, *41*, 10304.
21. Eriksson, A.; Siobhan, A.; Westermark, B.; Heldin, C. H.; Claesson-Welsh, L. *EMBO J*. **1992**, *11*, 543.
22. Josses, C.; Carron, C.; Boureux, A.; Quang, C. T.; Oury, C.; Dusanter-Fourt, I.; Charon, M.; Levin, J.; Bernard, O.; Ghysdael, A. *EMBO J*. **1997**, *16*, 69.
23. Claesson-Welsh, L.; Eriksson, A.; Morén, A.; Severinsson, L.; Östman, A.; Betsholtz, C.; Heldin, C. H. *Mol. Cell. Biol*. **1998**, *8*, 3476.